Supplementary Information

Amino acids as Latent Curing Agents and their Application in Fully Bio-based Epoxy Resins

Zhen Yu[1,2], Songqi Ma[1]*, Zhaobin Tang[1]*, Yanlin Liu[1], Xiwei Xu[1,3], Qiong Li[1,3], Kewei Zhang[2], Binbo Wang[1], Sheng Wang[1,3], Jin Zhu[1]

[1]Key Laboratory of Bio-based Polymeric Materials Technology and Application of Zhejiang Province, Laboratory of Polymers and Composites, Ningbo Institute of Materials Technology and Engineering, Chinese Academy of Sciences, Ningbo 315201, P. R. China;

[2] School of Materials Science and Engineering, Taiyuan University of Science and Technology, Shanxi 030024, P. R. China;

[3] University of Chinese Academy of Sciences, Beijing 100049, P. R. China;

*Corresponding authors: (Songqi Ma) E-mail masongqi@nimte.ac.cn, Tel 86-574-87619806; (Zhaobin Tang) tangzhb04@nimte.ac.cn.

Contents

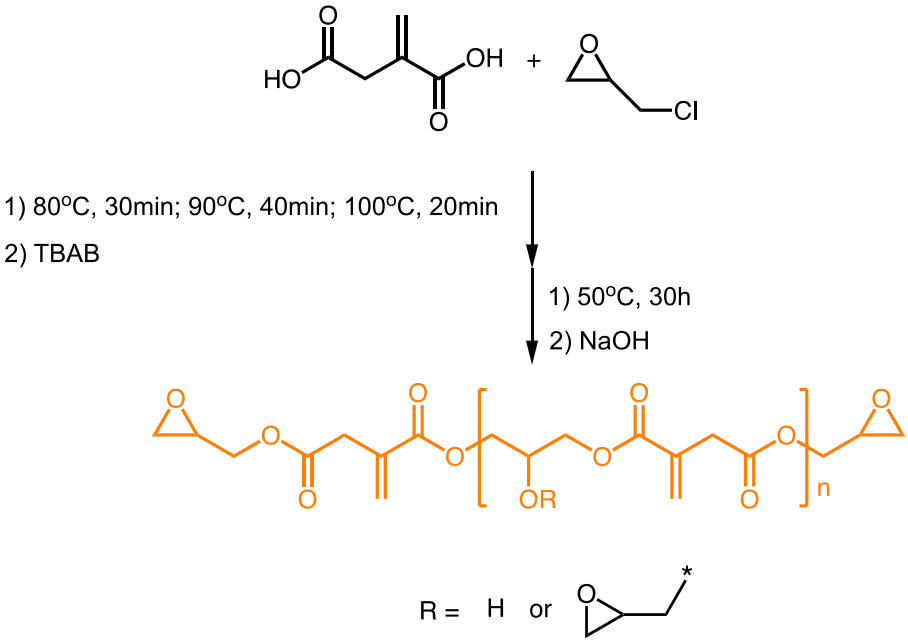

Scheme S1 Synthetic route of EIA.

Fig. S1 Digital photo of PDA-MAH.

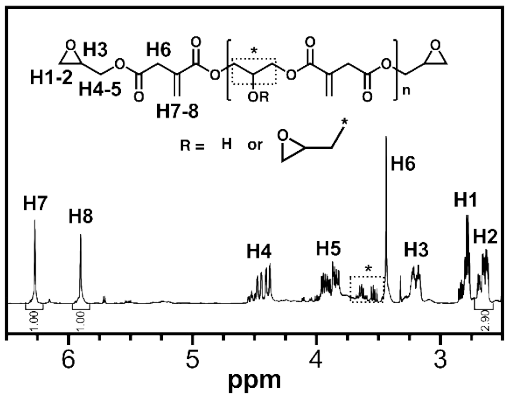

Fig. S2 ^{1}H NMR spectrum of EIA.

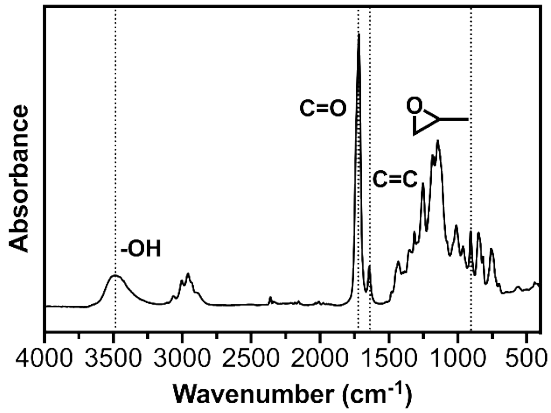

Fig. S3 FTIR spectrum of EIA.

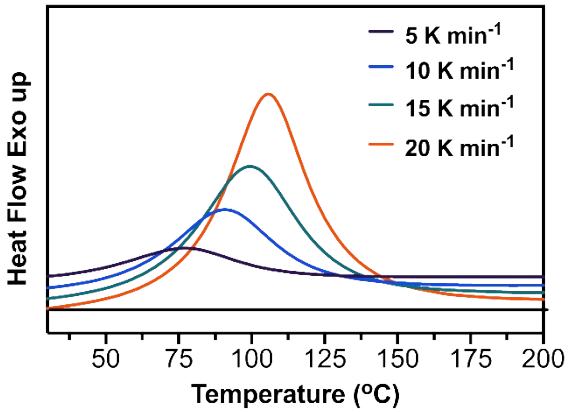

Fig. S4 Curing curves for DER331/PDA at different heating rates.

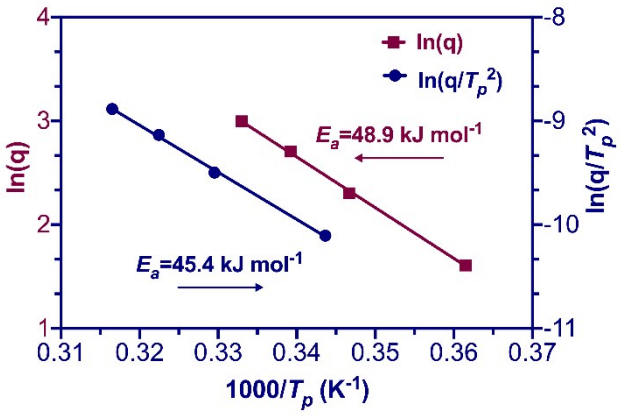

Fig. S5 ln$q$ and ln(q/T_p^2) as a function of 1000/T_p for DER331/PDA based on Ozawa and Kissinger's theories.

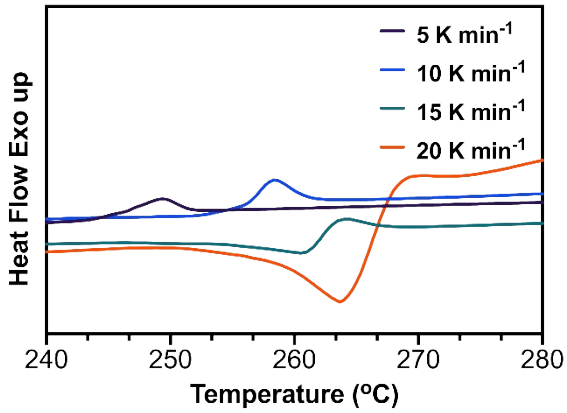

Fig. S6 Curing curves of DER331/Gly at different heating rates.

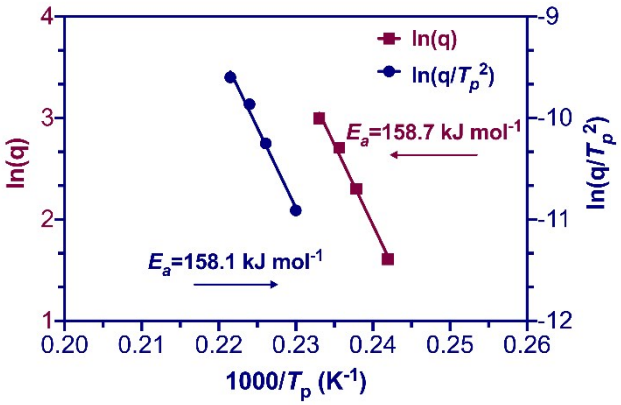

Fig. S7. ln$q$ and ln(q/T_p^2) as a function of 1000/T_p for DER331/Gly based on Ozawa and Kissinger's theories.

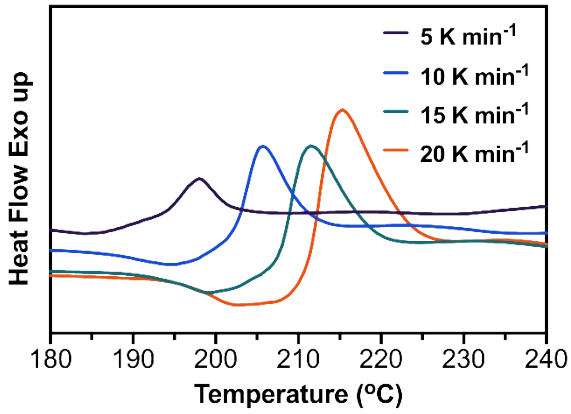

Fig. S8. Curing curves of DER331/Glu at different heating rates.

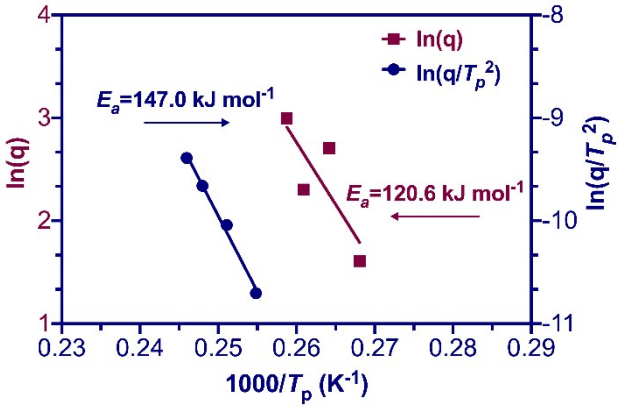

Fig. S9 ln$q$ and ln(q/T_p^2) as a function of 1000/T_p for DER331/Glu based on Ozawa and Kissinger's theories.

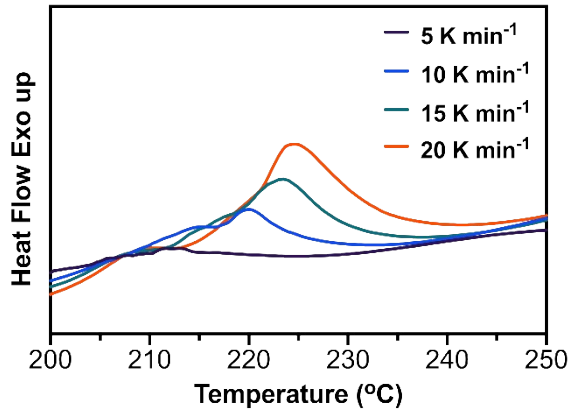

Fig. S10 Curing curves of DER331/Lys at different heating rates.

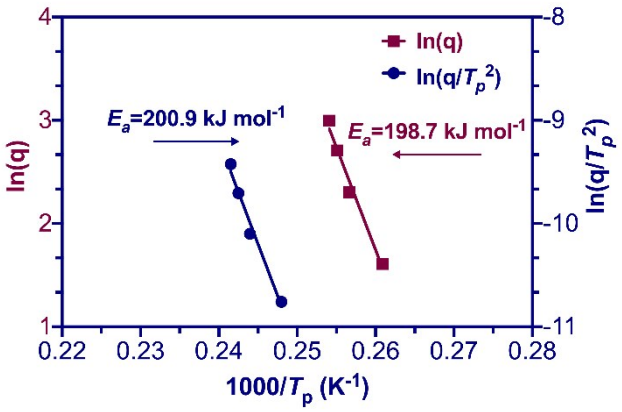

Fig. S11 ln$q$ and ln(q/T_p^2) as a function of 1000/T_p for DER331/Lys based on Ozawa and Kissinger's theories.

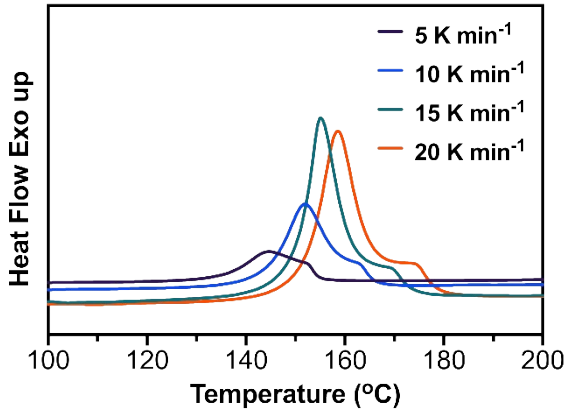

Fig. S12 Curing curves of DER331/AAD at different heating rates.

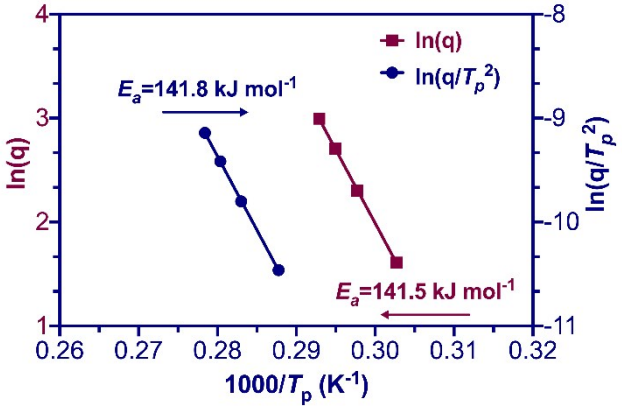

Fig. S13 ln$q$ and ln(q/T_p^2) as a function of 1000/T_p for DER331/AAD based on Ozawa and Kissinger's theories.

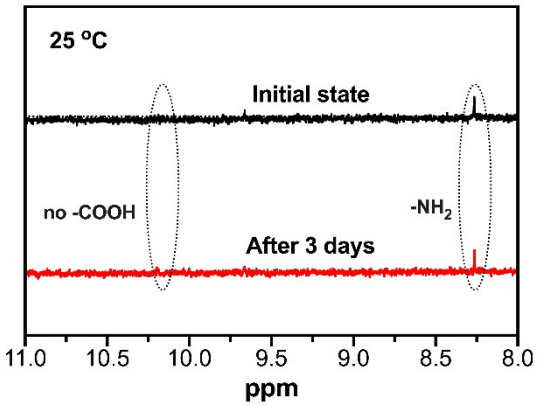

Fig. S14 ^{1}H NMR spectra of small molecule model system after storage at room temperature for 3 days.

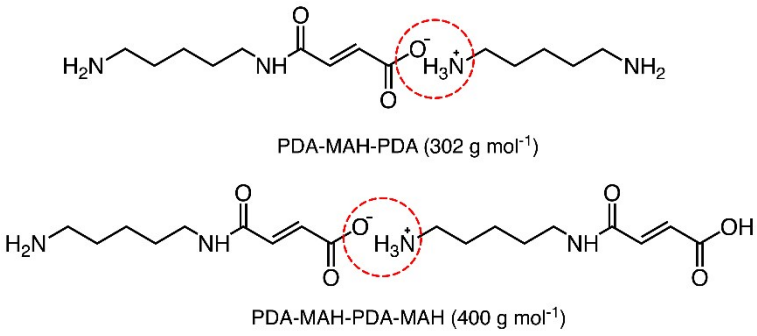

Fig. S15 Chemical stuctures of PDA-MAH-PDA and PDA-MAH-PDA-MAH.

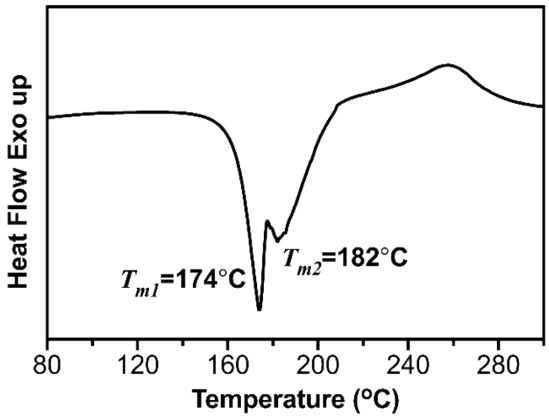

Fig. S16 DSC curve of PDA-MAH.

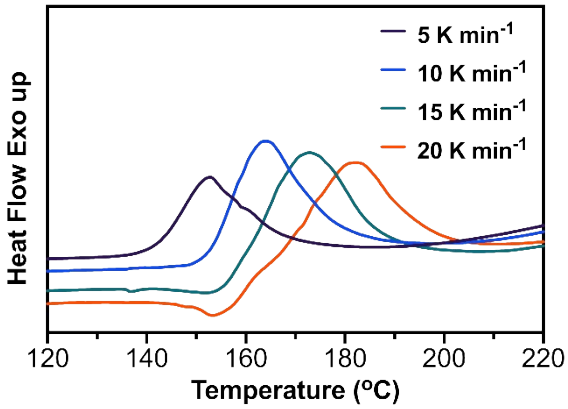

Fig. S17 Curing curves of DER331/PDA-MAH at different heating rates.

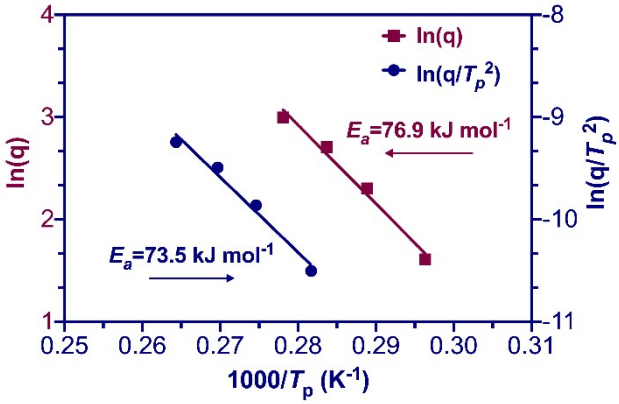

Fig. S18 ln$q$ and ln(q/T_p^2) as a function of 1000/T_p for DER331/PDA-MAH based on Ozawa and Kissinger's theories.

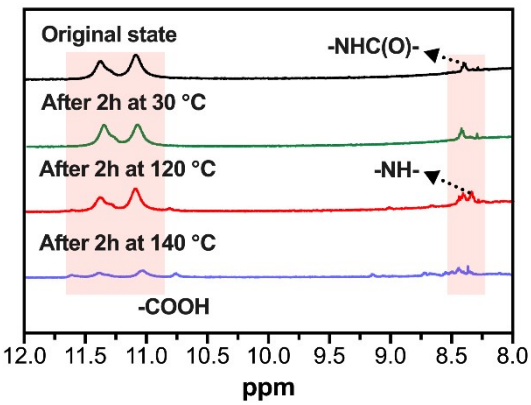

Fig. S19 ^{1}H NMR spectra of PDA-MAH and BGE models for small molecules.

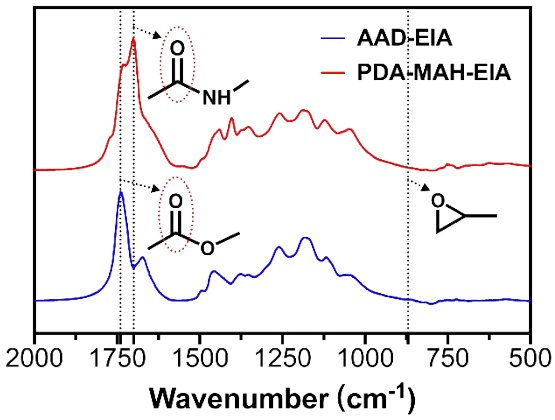

Fig. S20 FTIR spectra of PDA-MAH-EIA and AAD-EIA at room temperature.

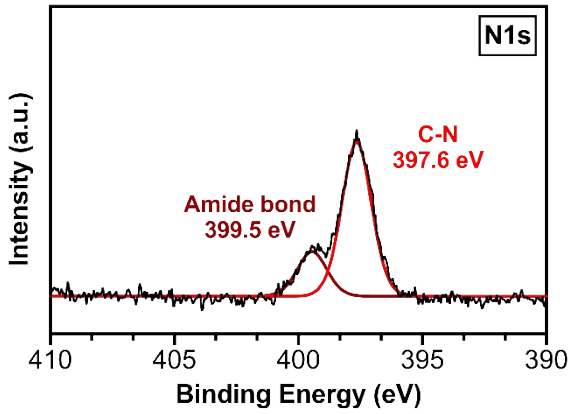

Fig. S21 XPS spectrum of PDA-MAH-EIA.

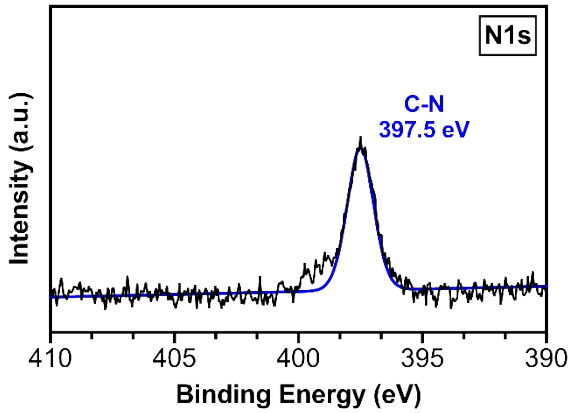

Fig. S22 XPS spectrum of AAD-EIA.

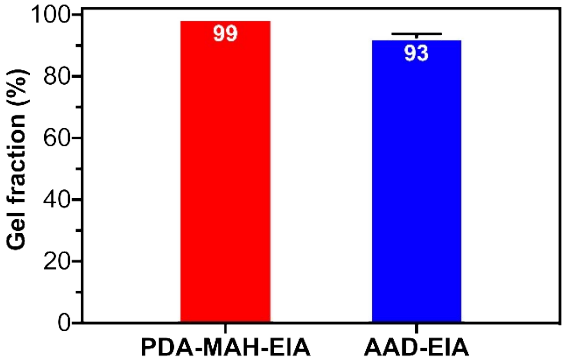

Fig. S23 Gel fraction of PDA-MAH-EIA and AAD-EIA.

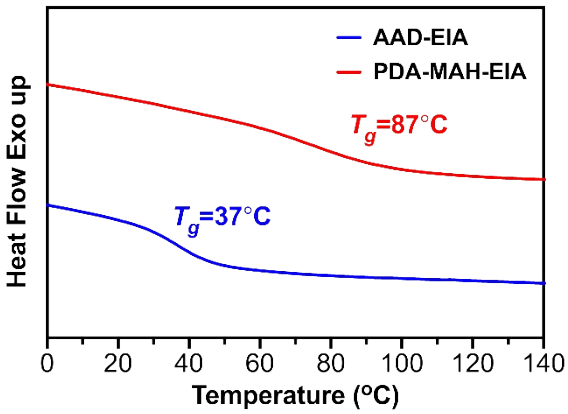

Fig. S24 DSC curves of PDA-MAH-EIA and AAD-EIA.

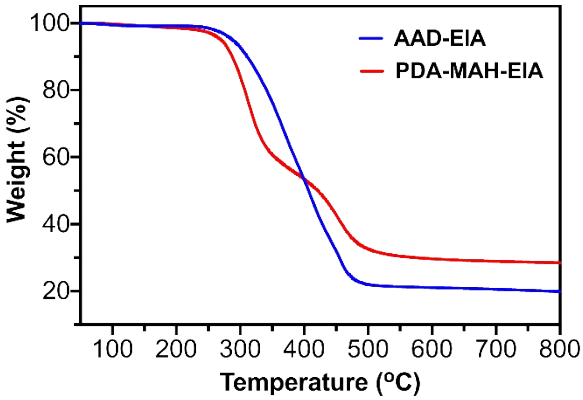

Fig. S25 TGA curves of PDA-MAH-EIA and AAD-EIA.

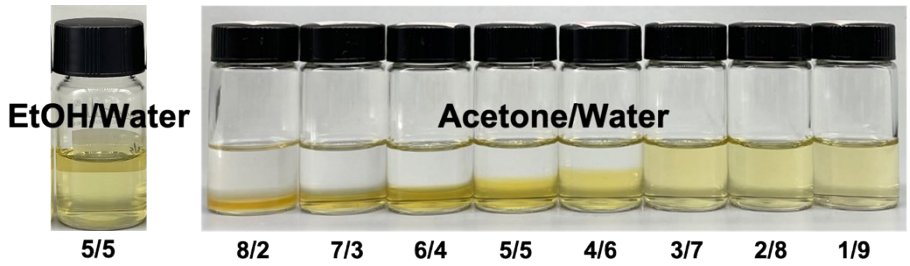

Fig. S26 Digital Photos of PDA-MAH-EIA after degradation.

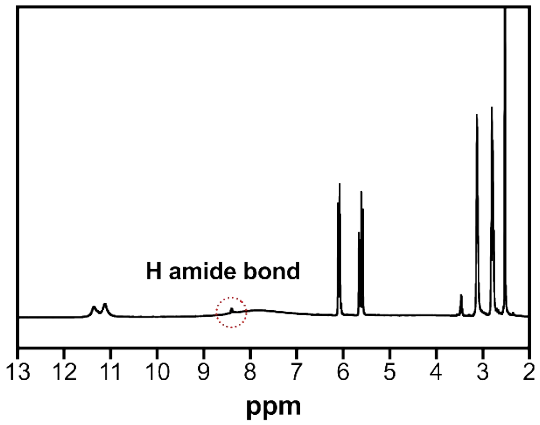

Fig. S27 ^{1}H NMR spectrum of PDA-MAH with DMSO-d_6 as solvent.

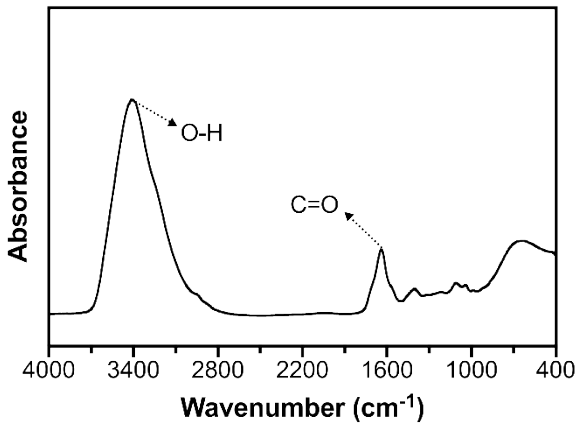

Fig. S28 FTIR spectrum of degradation products of PDA-MAH-EIA.

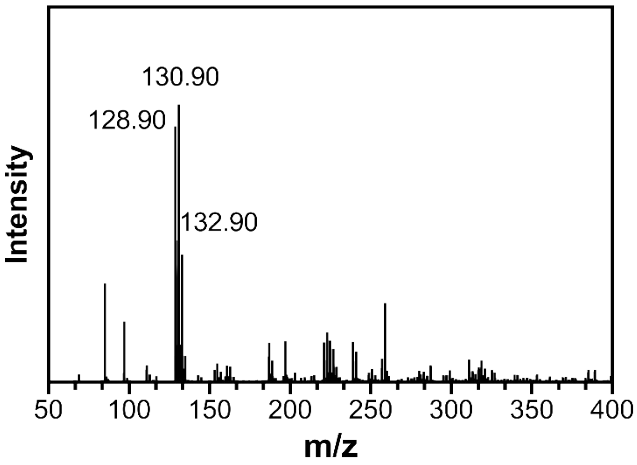

Fig. S29 TOF-MS spectrum of degradation products of PDA-MAH-EIA.

Table S1 The peak temperature (T_p), onset temperature (T_o) and activation energy (E_a) of curing reaction for different curing systems at different heating rate

DER331/curing agents	E_a (ln$q$)	E_a (ln(q/T_p^2))	5 ℃/min		10 ℃/min		15 ℃/min		20 ℃/min	
	kJ/mol	kJ/mol	T_o	T_p	T_o	T_p	T_o	T_p	T_o	T_p
DER331/PDA	48.9	45.4	49	77	59	92	66	100	73	107
DER331/Gly	158.7	158.1	237	250	253	259	263	264	267	270
DER331/Glu	120.6	147.0	194	199	203	206	209	212	212	216
DER331/Lys	198.7	200.9	185	212	193	220	197	223	200	225
DER331/AAD	141.5	141.8	135	145	142	152	147	156	150	159
DER331/PDA-MAH	76.9	73.5	142	154	153	165	161	173	168	182